A low-cost multichannel Thomson scattering system for CDX-U

T. Munsat and B. LeBlanc
Plasma Physics Laboratory, Princeton University, Princeton, New Jersey 08543

(Presented on 9 June 1998)

A multichannel Thomson scattering system has been developed for the CDX-U spherical torus. The system is designed for $10\ \text{eV} < T_e < 400\ \text{eV}$, $n_e > 10^{18}\ \text{m}^{-3}$, which includes typical and predicted central and edge conditions in CDX-U. The system uses two laser passes to double the scattered photons from a 5 J ruby laser. The beam path is vertical through the ~66 cm (elongated) diameter of the plasma and is movable in the major-radial direction, enabling coverage of nearly 70% of the major-radial plasma extent. Twelve channels over the vertical minor radius provide ~2.5 cm spatial resolution. The main collecting lens, located 45 cm from the laser beamline, provides high solid angle ($\Delta\Omega \sim 0.01$) light collection using a 15 cm diam lens. The system makes maximum usage of an optically fast ($f/1.8$) compact imaging spectrometer. An intensified charge coupled device with a GaAs photocathode provides quantum efficiency of ~20% at 6943 Å. The combination of plasma access, multiple beam passes, high-throughput spectrometer, and high quantum efficiency detector provide for very high total photon statistics in a relatively simple and inexpensive system. © *1999 American Institute of Physics.* [S0034-6748(99)55401-4]

I. INTRODUCTION

In the past, due to performance and cost issues, multichannel Thomson scattering systems (TVTS systems[1]) using imaging detectors were not feasible for smaller plasma physics experiments such as CDX-U. As smaller experiments become more sophisticated, though, profile information becomes increasingly valuable, while at the same time technological advances and component availability make TVTS systems much more affordable and manageable. This article describes the major components and innovative aspects of the CDX-U TVTS system, presently under construction.

II. OVERVIEW

CDX-U is a spherical torus (ST) with $R \approx 34$ cm, $R/a \geqslant 1.5$, $\kappa \leqslant 1.6$. The OH and magnetics power systems are presently being upgraded, enabling approximately a factor of 2 increase in both toroidal field (to 2.3 kG on axis) and expected plasma current (to 150 kA), as well as a several-fold increase in discharge flattop duration (to 20–25 ms). Typical plasma parameters with the previous power system include $n_e(0) \approx 10^{19}\ \text{m}^{-3}$, $T_e(0) \approx 100\ \text{eV}$. The TVTS system is designed to measure $10\ \text{eV} \leqslant T_e \leqslant 400\ \text{eV}$, $n_e \geqslant 10^{18}\ \text{m}^{-3}$.

In order to increase the amount of scattered light from the relatively low-density plasma, the laser beam passes through the plasma twice, along nearly overlapping paths. The system provides 12 spatial points along an elongated minor radius of the plasma, corresponding to a 2.5 cm spatial resolution over one half of the plasma cross section. The scattered light distribution is sampled at five spectral points.

III. LASER PATH

The system uses a 5 J ruby laser, housed on a sliding framework which is movable in the major-radial direction (Fig. 1). The beam passes vertically down through the

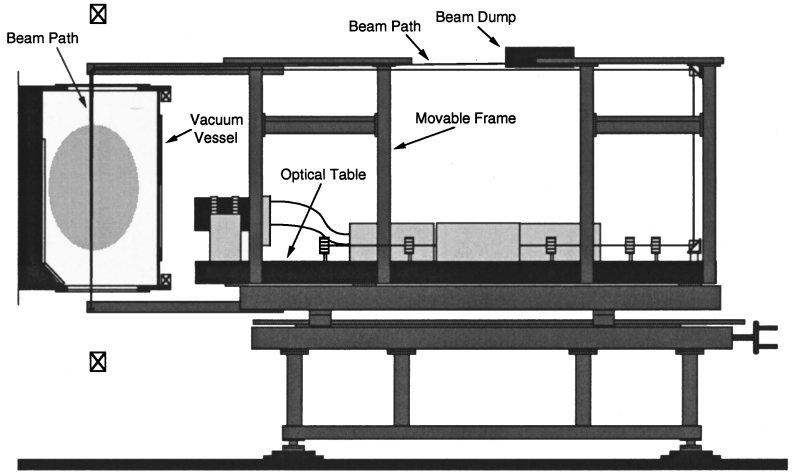

FIG. 1. CDX-U TVTS system with half cross section of vacuum vessel. Visible are two-pass vertical beam path, beam dump, and optical table housing laser and all collection optics.

plasma, is reflected by a spherical mirror below the vacuum vessel, and passes back through the plasma, to be steered out to an external beam dump. The steering optics and beam dump are located outside of the field of view of the collecting optics.

The beam enters and exits the vacuum vessel through two antireflection (AR) coated windows (tilted by 7°, to avoid cavity modes). The windows have over 30 cm clear aperture in the major-radial direction, allowing for coverage of nearly 70% of the major-radial plasma extent (Fig. 2). The movable optical table allows for two-dimensional (2D) scanning of the plasma cross section, allowing for reconstruction of the plasma shape, and identification of some asymmetries.

The laser itself was previously used in the Tokamak Fusion Test Reactor (TFTR) TVTS system.[2] The CDX-U system uses a modified version of the laser, eliminating the final amplification head and expanding the oscillator cavity. The CDX-U system will use three ruby heads and a longer cavity to expand the pulse length to ~50 ns. Because of the short (50 ns) gate duration, background light is not expected to significantly deteriorate the scattered photon signal-to-noise ratio.

The two-pass system doubles the number of scattered photons per joule of laser energy, thus lessening the laser energy requirements. Technical limitations inherent to the CDX-U machine make this an essential feature of the system. In order to avoid the CDX-U poloidal field coils with a vertical beam path, it is necessary to place steering optics very close to the plasma scattering volume. Damage threshold (power-density) limits on the optical coatings of these elements, along with optical (aspect-ratio) requirements of the plasma scattering volume itself, place lower *and* upper limits on the width of the beam as it comes in contact with the optics and passes through the plasma. With a two-pass system, the design requirements on beam power density can be met while retaining sufficient photons for measurements. The beam is $\geqslant$6 mm in diameter at all optical surfaces, resulting in power density on the optics $\leqslant$350 MW/cm^2 for a uniform (top-hat) beam profile, nearly an order of magnitude below damage threshold specs. The beam is also $\leqslant$4 mm in diameter over the entire plasma scattering volume, which is fully imaged by the collection optics. Though an increase in the number of laser passes (to more than two) would further increase the level of scattered light, we have chosen to use two passes based on the simplicity of the optical design.

IV. LIGHT COLLECTION

The collection optics include the main collection lens, an array of plastic fiberoptic bundles, a high-dispersion spectrometer, and an intensified charge coupled device (ICCD) camera with GaAs photocathode. This combination of components was chosen to be simple, cost effective, and modular.

The main collecting lens [Fig. 3(a)] is a custom designed five-element, 10.5 cm focal-length lens covering 34° at $f/2$, magnification 0.23. Results from ray-tracing analysis using the OSLO[3] code [Fig. 3(b)] indicate a 0.1 mm rms spot size over the entire field of view. The five glass elements are all

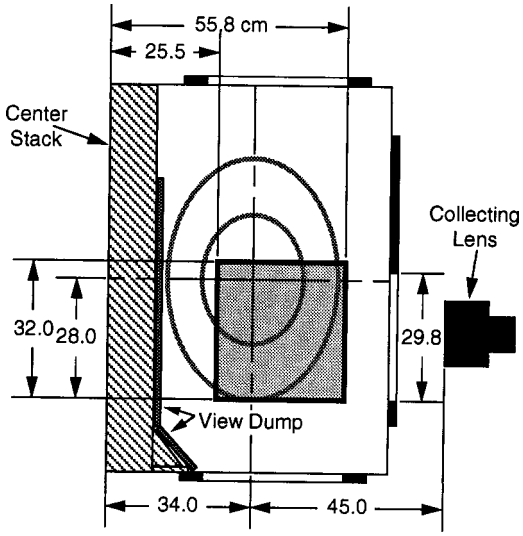

FIG. 2. Close-up of vacuum vessel cross section with TVTS coverage indicated. One elongated plasma radius is imaged, and the entire system is scannable over nearly 70% of the major-radial plasma extent.

stock catalog items, BK7 or fused silica, with diameters ranging from 5–15 cm. The use of stock elements allows for a very inexpensive lens system; the combined price of all five AR coated glass elements was roughly equal to the cost of the custom lens mount that holds them.

The lens is 45 cm from the beamline, and images 32 cm of the beam onto an array of plastic optical fibers arranged on a curved focal plane. Though the front lens element is $\phi = 15$ cm, the nonvignetted collection area is $\phi = 5.2$ cm, which provides $\Delta\Omega = 0.01$ at the optical axis, 0.008 at the edge of field. Despite the fact that the collection area is smaller than on other TVTS systems, close plasma access allows for a collection solid angle comparable to other systems.[1]

An array of square plastic fibers is used to rearrange the image of the beam into the entrance slit of the spectrometer [Fig. 4(a)]. Plastic fibers are much less expensive than custom quartz fiber bundles, and are not overly lossy for short transmission distances. Though the plastic-fiber lossiness peaks exactly in the wavelength region of interest (700–750 nm), even at worst the loss is $\leqslant$1.8 dB/m. For the 25 cm fiber length used in this system, this translates to 90% transmission. By comparison, quartz fiber bundles can be extremely transmissive over long distances, but are subject to finite packing and cladding fractions which typically limit transmission to $\leqslant$60%. Plastic fibers, though much lossier over long distances, can be produced with square cross section, increasing the packing fraction to essentially 1. Fiber cladding takes up ~15% of the cross sectional area. As shown in Fig. 4(b), standard fiber sizes have been arranged to provide custom bundle dimensions.

In order to cover the full plasma half radius while still fitting all of the fibers into the 20 mm entrance slit of the spectrometer, the fiber bundles are arranged with gaps between them, so that the fibers sample the entire beam length but only collect 50% of the scattered light [Fig. 4(a)]. The

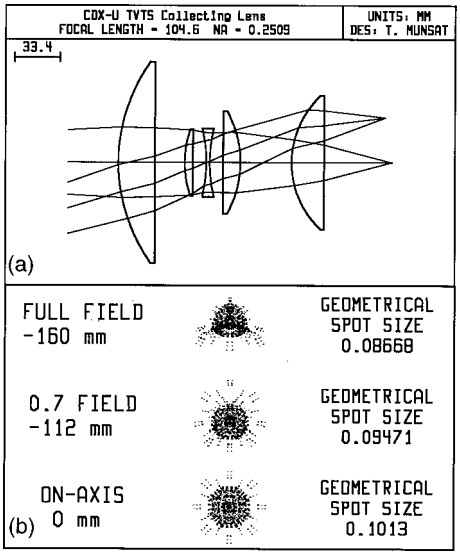

FIG. 3. (a) Five-element collection lens, with center and edge image-focus shown. All elements are stock catalog items. (b) Ray-trace spot-size analysis. Spot size is ≤ 0.1 mm over the full field of view.

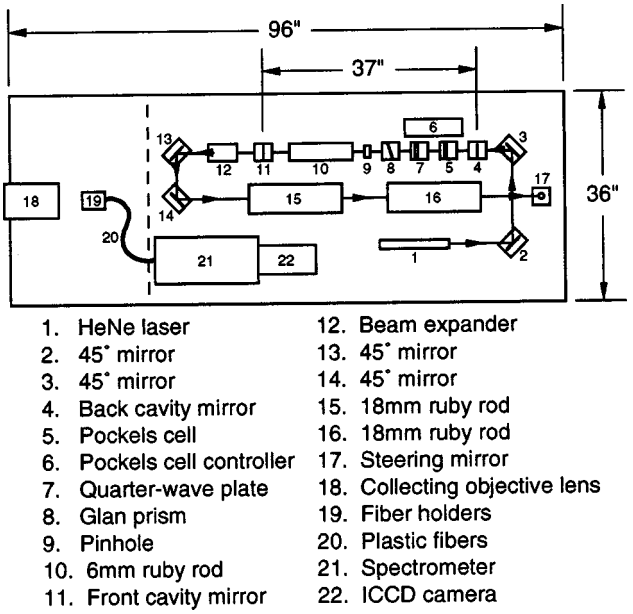

FIG. 5. Optical table layout. All laser components, collection optics, spectrometer, and camera fit onto a 3 ft×8 ft optical table.

fiber tips are mounted in a modular holder, alternating fiber bundles with ''blanks,'' so that the fiber bundles and the blanks can be rearranged to observe a smaller region of the plasma at higher resolution. This arrangement also provides a simple upgrade path to double the spatial resolution with the purchase of a second spectrometer and camera, by merely filling in the blanks with fiber bundles. Four channels record background and scattered light from locations distributed across the plasma height, and are recorded simultaneously with the signal channels (see Fig. 4). A 71 cm×7.5 cm view dump made of nonmagnetic stainless-steel razor blades is located on the vacuum vessel center stack.

Collected light is dispersed with an $f/1.8$ spectrometer which uses a volume-holographic transmission grating sandwiched between two prisms.[4] This spectrometer was chosen for its combination of high light throughput and compactness. The input light is pre-filtered with a holographic rejection filter tuned to the ruby line. Wavelengths in the range $680<\lambda<700$ nm are rejected by 10^6. The spectrometer disperses ~2.5 nm/mm onto a 10.8 mm wide detector, covering 700–727 nm.

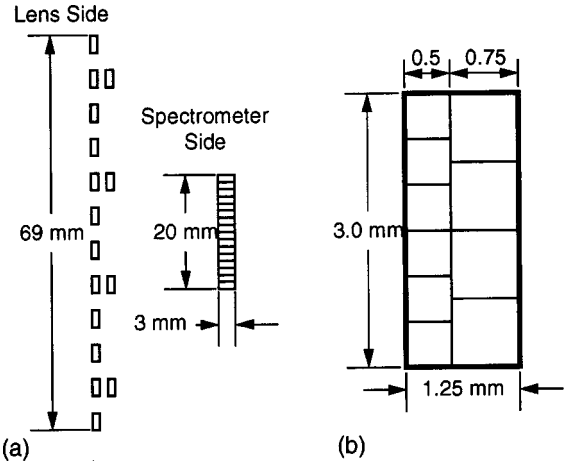

FIG. 4. (a) Fiber-bundle tips, with rearrangement between the lens-image side and at the spectrometer entrance slit shown. Gaps between bundles at the lens side allow for full beamline coverage while still fitting channels into the spectrometer entrance slit. (b) Close-up of a single fiber bundle. Custom dimensions are attainable with stock (0.5 and 0.75 mm) square-fiber sizes.

The detector used is an ICCD camera previously used for the edge TVTS system on TFTR.[5] The intensifier uses a GaAs photocathode which provides ~20% quantum efficiency in the 700 nm range. Noise implicit to signal amplification and digitization is expected to reduce the ''detective quantum efficiency'' to ~10%.

Because of the compactness of the system components, the entire system fits onto an 8 ft×3 ft optical table (Fig. 5), greatly simplifying alignment and radial scanning. As the table is moved in the major-radial direction, the laser, all of the beam optics, and all of the collection optics are moved together, preserving the alignment.

V. SYSTEM PERFORMANCE

The quality of scattered spectra at any particular location in the plasma will be critically dependent on both n_e and T_e at that location. In order to accurately model system performance, sample n_e and T_e profiles were used that correspond to conservative estimates of expected CDX-U performance, and TVTS performance was modeled as a function of position in the plasma. In the model $n_e(0)=10^{19}$ m^{-3}, $n_e(a)=10^{18}$ m^{-3}, $T_e(0)=120$ eV, and $T_e(a)=12$ eV (a here refers to the plasma edge in the vertical direction, as seen by the TVTS system).

The number of photoelectrons produced per pixel by scattered light is given by[6]

$$N_{\mathrm{pe}} \cong N_i(\eta T) n_e r_0^2 L(\Delta\Omega)\left\{\frac{1}{\lambda_i \delta\sqrt{\pi}}\exp\left[-\frac{(\lambda_s-\lambda_i)^2}{\lambda_i^2\delta^2}\right]\Delta\lambda\right\},$$

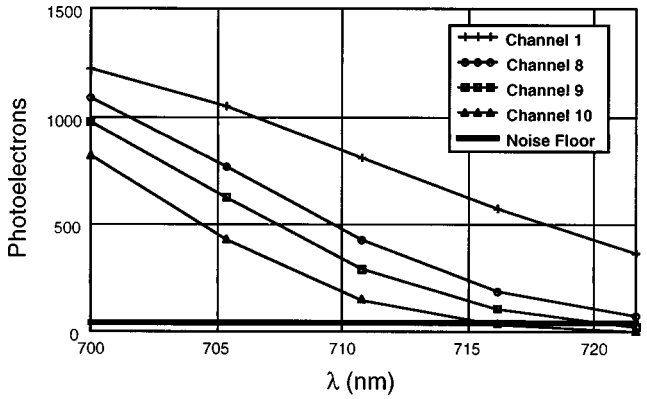

FIG. 6. Modeled spectra for four selected spatial channels. Shown are channels 1 (center), 8, 9, and 10 (near edge). Channels 11 and 12 (edge, not shown) have fewer than three spectral points above the noise floor.

where $N_i(r)$ is the number of incident photoelectrons (10 J $\approx 3.5\times 10^{19}$), η is the effective photocathode quantum efficiency (~ 0.1), T is the transmission of the optical train (~ 0.3), $n_e(r)$ is the electron density, r_0 is the classical electron radius, L is the laser beamlength sampled per pixel (1.25 cm), $\Delta\Omega$ is the collection solid angle (0.010 on the optical axis, 0.008 at edge of field), $\lambda_{s,i}$ are the scattered and incident wavelengths, $\Delta\lambda$ is the wavelength interval sampled per pixel (54 Å). The variable δ differs from Ref. 6 in this system because of the double-pass beam path through the plasma. Light will be scattered from both the down-going and up-going beams, and the two resulting scattering angles must be accounted for

$$\delta = \sqrt{\frac{8kT_e}{m_e c^2}}\left[\frac{1}{2}\sin(\theta_{s1}) + \frac{1}{2}\sin(\theta_{s2})\right],$$

where $\theta_{s1,2}$ are the angles between the down, up-going beam and the scattering direction. (θ_s ranges between 72° and 108°.) Note that N_i corresponds to the total number of incident photons, summed over the two laser passes. In practice, the ratio of down-going to up-going beam power (represented by the two factors of $\frac{1}{2}$ in the scattering formula) may be slightly different than 1 due to finite power absorption at the reflecting mirror.

Taking 50 photoelectrons per pixel as the expected noise floor, the sample T_e and n_e profiles provide full five-point spectra over spatial channels 1–7, four-point spectra over channels 8 and 9, a three-point spectrum in channel 10, and a two-point spectrum in channel 11. Channel 12 (corresponding to the edge values of n_e and T_e) only has signal exceeding the noise floor in the first spectral channel. Note that this does not explicitly rule out measuring T_e down to the edge value, but higher n_e is required in order to produce a readable signal in the outer spectral channels. As described above, the fiber bundles can be moved to cover different regions of the plasma as needed. Figure 6 shows the expected two-pass spectra (photoelectrons versus wavelength) for several selected spatial channels.

In order to model the expected error in the T_e and n_e measurements due to photon noise, artificial Poisson-type noise was added to the predicted photon signals. The error was then propagated through the extraction of T_e and n_e from nonlinear least-squares fits to the photon spectra. (A nonlinear least-squares fit is required because the two-pass system produces bi-maxwellian spectra.) For the central channel $\sigma(T_e) = 4.5$ eV (3.8%) and $\sigma(n_e) = 1.6\times 10^{17}$ m^{-3} (1.6%). For channel 10 (near edge) $\sigma(T_e) = 2.4$ eV (5.1%) and $\sigma(n_e) = 1.2\times 10^{17}$ m^{-3} (3.1%).

VI. DISCUSSIONS

Through the use of several novel design features and by taking advantage of advances in spectrometer and fiberoptic technology, increased availability and selection of off-the-shelf optical components, and the lower cost of imaging detectors, we hope to demonstrate that TVTS is a realistic option for small experiments such as CDX-U. The two-pass laser system, custom-designed collection lens, plastic fiberoptic bundles, high-throughput spectrometer, and high quantum-efficiency ICCD all combine to produce very high total photon statistics in a relatively simple and inexpensive system.

ACKNOWLEDGMENTS

This work was supported by U.S. DOE Contract No. DE-AC02-76-CHO3073. The authors would like to thank D. Johnson and D. Long for their invaluable help.

[1] D. Johnson, N. Bretz, D. Dimock, B. Grek, D. Long, R. Palladino, and E. Tolnas, Rev. Sci. Instrum. **57**, 1856 (1986).
[2] D. Johnson, D. Dimock, B. Grek, D. Long, D. McNeill, R. Palladino, J. Robinson, and E. Tolnas, Rev. Sci. Instrum. **56**, 1015 (1985).
[3] Sinclair Optics, Rochester, NY.
[4] H. Owen, D. E. Battey, M. J. Pelletier, and J. B. Slater, Proc. SPIE **2406**, 260 (1995).
[5] D. Johnson, B. Grek, D. Dimock, R. Palladino, and E. Tolnas, Rev. Sci. Instrum. **57**, 1810 (1986).
[6] N. Bretz, D. Dimock, V. Foote, D. Johnson, D. Long, and E. Tolnas, Appl. Opt. **17**, 192 (1978).